Structural elements in the Girk1 subunit that potentiate G protein–gated potassium channel activity

Nicole Wydeven, Daniele Young, Kelsey Mirkovic, and Kevin Wickman[1]

Department of Pharmacology, University of Minnesota, Minneapolis, MN 55455

Edited* by David E. Clapham, Howard Hughes Medical Institute, Children's Hospital Boston, Boston, MA, and approved November 15, 2012 (received for review July 13, 2012)

G protein–gated inwardly rectifying K^+ (Girk/K_{IR}3) channels mediate the inhibitory effect of many neurotransmitters on excitable cells. Girk channels are tetramers consisting of various combinations of four mammalian Girk subunits (Girk1 to -4). Although Girk1 is unable to form functional homomeric channels, its presence in cardiac and neuronal channel complexes correlates with robust channel activity. This study sought to better understand the potentiating influence of Girk1, using the $GABA_B$ receptor and Girk1/Girk2 heteromer as a model system. Girk1 did not increase the protein levels or alter the trafficking of Girk2-containing channels to the cell surface in transfected cells or hippocampal neurons, indicating that its potentiating influence involves enhancement of channel activity. Structural elements in both the distal carboxyl-terminal domain and channel core were identified as key determinants of robust channel activity. In the distal carboxyl-terminal domain, residue Q404 was identified as a key determinant of receptor-induced channel activity. In the Girk1 core, three unique residues in the pore (P) loop (F137, A142, Y150) were identified as a collective potentiating influence on both receptor-dependent and receptor-independent channel activity, exerting their influence, at least in part, by enhancing mean open time and single-channel conductance. Interestingly, the potentiating influence of the Girk1 P-loop is tempered by residue F162 in the second membrane-spanning domain. Thus, discontinuous and sometime opposing elements in Girk1 underlie the Girk1-dependent potentiation of receptor-dependent and receptor-independent heteromeric channel activity.

ion channel | electrophysiology | mutagenesis | baclofen

Many neurotransmitters inhibit neurons by activating receptors linked to heterotrimeric GTP-binding proteins (G proteins). A prototypical effector in such signaling pathways is the G protein–gated inwardly rectifying K^+ (Girk/K_{IR}3) channel (reviewed in ref. 1). Girk channels are tetramers, with each subunit possessing intracellular N and C termini and a core domain containing two transmembrane segments, two short extracellular loops, and a hydrophobic domain (pore loop, referred to hereafter as P-loop) that contributes to the pore and K^+ selectivity filter. Four mammalian *Girk* genes have been identified (*Girk1* to *Girk4*). The classic mode of Girk channel activation involves the direct binding of Gβγ subunits, which stabilizes a low-affinity interaction between the channel and phosphatidylinositol 4,5-bisphosphate (PIP_2).

Girk2 plays a key role in neuronal Girk channel formation (e.g., ref. 2). Overlapping expression patterns and the impact of *Girk2* ablation on *Girk1* expression, however, argue that most neuronal Girk channels contain both Girk1 and Girk2 (3, 4). In support of this contention, *Girk1* ablation yields a near-complete loss of Girk-dependent signaling in neurons that express Girk1 (e.g., ref. 5). These findings are surprising because Girk2 forms functional homomers in expression systems that exhibit G protein–dependent gating, K^+ selectivity, and inward rectification (6). Moreover, Girk2 homomers have been identified in midbrain dopamine neurons (7). Nevertheless, work in expression systems has shown clearly that Girk1 potentiates receptor-dependent and receptor-independent currents when coexpressed with Girk2 or Girk4 (6, 8–10).

Many studies have provided insight into the structural basis of channel regulation by G proteins, PIP_2, and Na^+, as well as channel-gating mechanisms (1). Most of the relevant structural elements, however, are well conserved across Girk subunits and, thus, cannot explain how Girk1 potentiates Girk signaling. Here, we sought insights into the structural elements unique to Girk1 that potentiate Girk channel activity, using mutagenesis approaches exploiting insights from previous biochemical and crystallography studies.

Results

Girk1-Dependent Potentiation of $GABA_B$ Receptor–Girk Signaling. HEK cells expressing the $GABA_B$ receptor ($GABA_BR$) subunits $GABA_BR1$ and $GABA_BR2$, along with epitope-tagged Girk1 and Girk2, exhibited large currents in response to a saturating concentration of the $GABA_BR$ agonist baclofen, as well as receptor-independent or basal (Ba^{2+}-sensitive) whole-cell currents (Fig. 1 *A* and *B*). In contrast, currents in cells expressing $GABA_BR$ and Girk2 were small. Consistent with previous observations (11, 12), pretreatment of cells expressing the Girk1/Girk2 heteromer with pertussis toxin, which uncouples Gi/o G proteins from activated receptors, eliminated the baclofen-induced but not basal current (Fig. 1*B*). Thus, Girk1 potentiates Girk currents in both receptor-dependent and receptor-independent manners. Girk2 levels at the cell surface measured using a biotinylation approach were not significantly different with or without Girk1 present (Fig. 1 *C* and *D*). Moreover, the ratio of surface-to-total Girk2 protein was unaltered, indicating that Girk1 does not impact the surface trafficking of Girk2-containing channels.

We also examined the impact of *Girk1* ablation on $GABA_BR$-Girk signaling in mouse hippocampal cultures. *Girk1* ablation yielded a dramatic reduction (~80%) in baclofen-induced currents in large pyramidal-shaped neurons (Fig. S1*A*). Interestingly, the small residual currents in neurons from *Girk1*$^{-/-}$ mice correlated with a significant increase in *$GABA_BR1$* and *Girk2* expression (Fig. S1*B*). There was no difference, however, in total or surface Girk2 protein levels in cultures from wild-type and *Girk1*$^{-/-}$ mice (Fig. S1*C*). Collectively, these data indicate that the potentiating effect of Girk1 on Girk currents in heterologous and native systems is not attributable to increased protein levels or surface targeting of Girk2.

Influence of the Distal C Terminus. Multiple intracellular domains have been implicated in the binding of Gβγ to Girk subunits (1). These elements are highly conserved across Girk subunits, however, and, thus, cannot explain the potentiating influence of Girk1. Although the unique distal C-terminal Girk1 domain between residues 390–462 does not bind Gβγ directly, it has been shown to enhance the binding of the Girk1 C terminus to Gβγ (13). As such, we used a targeted deletion strategy to probe the functional relevance of this and surrounding domains (Fig. 2). The deletion mutants were expressed at levels comparable to Girk1 (Fig. S2 *A*

Author contributions: N.W. and K.W. designed research; N.W., D.Y., K.M., and K.W. performed research; K.W. contributed new reagents/analytic tools; N.W., D.Y., K.M., and K.W. analyzed data; and N.W. and K.W. wrote the paper.

The authors declare no conflict of interest.

*This Direct Submission article had a prearranged editor.

[1]To whom correspondence should be addressed. E-mail: wickm002@umn.edu.

This article contains supporting information online at www.pnas.org/lookup/suppl/doi:10.1073/pnas.1212019110/-/DCSupplemental.

www.pnas.org/cgi/doi/10.1073/pnas.1212019110

Downloaded at Palestinian Territory, occupied on December 18, 2021

www.manaraa.com

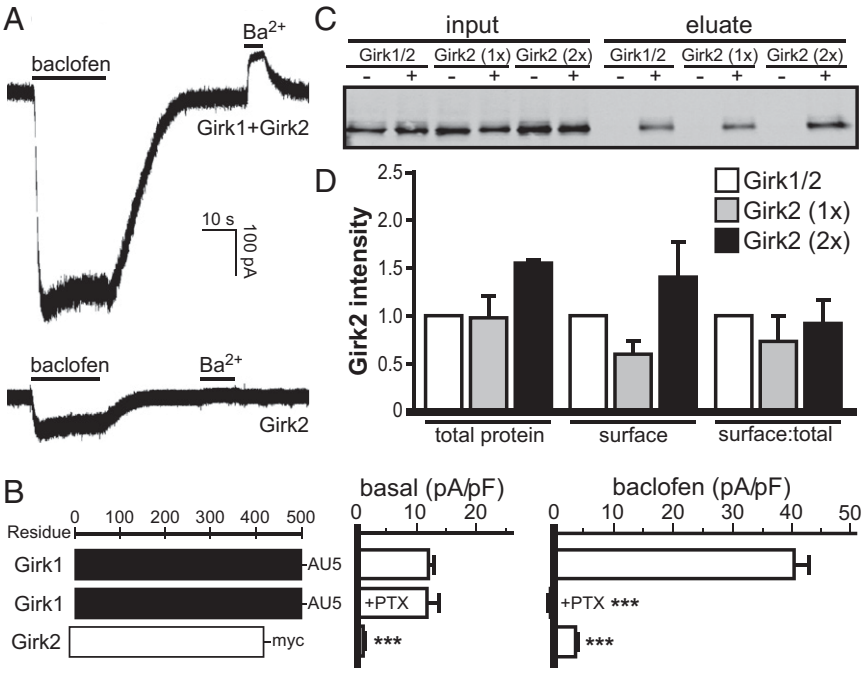

Fig. 1. Potentiating influence of Girk1. (*A*) Baclofen-induced and basal (Ba^{2+}-sensitive) currents, measured in a high-K^+ bath solution (25 mM) at a holding potential of −70 mV, in cells expressing $GABA_BR$ and either Girk1/Girk2 or Girk2 alone. Bars denote the duration of baclofen (100 μM) and Ba^{2+} (0.3 mM) applications. (*B*) Summary of currents measured in cells expressing Girk2 and $GABA_BR$, along with the subunit depicted on the left (n = 15–61 per group). Girk2 homomeric currents were measured in cells transfected with double (2×) the amount of Girk2 used in cells transfected with Girk1 and Girk2. A subset of cells expressing Girk1/Girk2 was pretreated (24 h) with pertussis toxin (PTX) (0.1 ng/mL). A significant impact of group was observed for basal ($F_{2,94}$ = 9.5; P < 0.001) and baclofen-induced ($F_{2,98}$ = 61.1; P < 0.001) currents. ***P < 0.001 vs. Girk1/Girk2. (*C*) Blot from a biotinylation experiment probing total and surface Girk2 protein levels in cells transfected with Girk1 and Girk2 (Girk1/2), Girk2 alone (1×), and Girk2 alone at twice the concentration (2×). (*D*) Quantification of biotinylation data (n = 3 separate experiments). No significant differences were detected between groups.

and *B*), and the protein levels and surface trafficking of Girk2 were comparable in cells expressing Girk1 or deletions (Fig. S2 *C–E*).

Basal and baclofen-induced currents were measured in cells transfected with Girk1 deletion constructs, Girk2, and $GABA_BR$ (Fig. 2*A*). The first construct tested (Girk1Δ462) revealed that the last 39 aa of Girk1 are not required for normal basal or $GABA_BR$-dependent Girk currents. Basal current for Girk1Δ409/Girk2 and Girk1Δ406/Girk2 heteromers was, however, significantly lower than those measured for Girk1/Girk2, whereas $GABA_BR$-dependent Girk currents were preserved. Further deletion (Girk1Δ399) correlated with a significant decrease in baclofen-induced Girk currents. Thus, structures between residues 409 and 462 uniquely support robust basal activity, whereas residues 399–406 are important for robust $GABA_BR$-dependent Girk currents.

A sharp distinction in baclofen-induced currents was observed for Girk1Δ406/Girk2 and Girk1Δ403/Girk2 heteromers. Mutation of the pertinent residues individually to alanine (Q404A, K405A, I406A), in the context of the Girk1Δ406 backbone, identified Q404 as a possible determinant of robust receptor-induced current (Fig. 2 *B* and *C*). Basal current observed with the Girk1(Q404A) mutation was smaller than Girk1Δ406, although this difference was not statistically significant.

We next engineered the Q404A mutation into full-length Girk1. Whereas basal activity was not different in cells expressing $GABA_BR$, Girk2, and either Girk1 or Girk1(Q404A), baclofen-

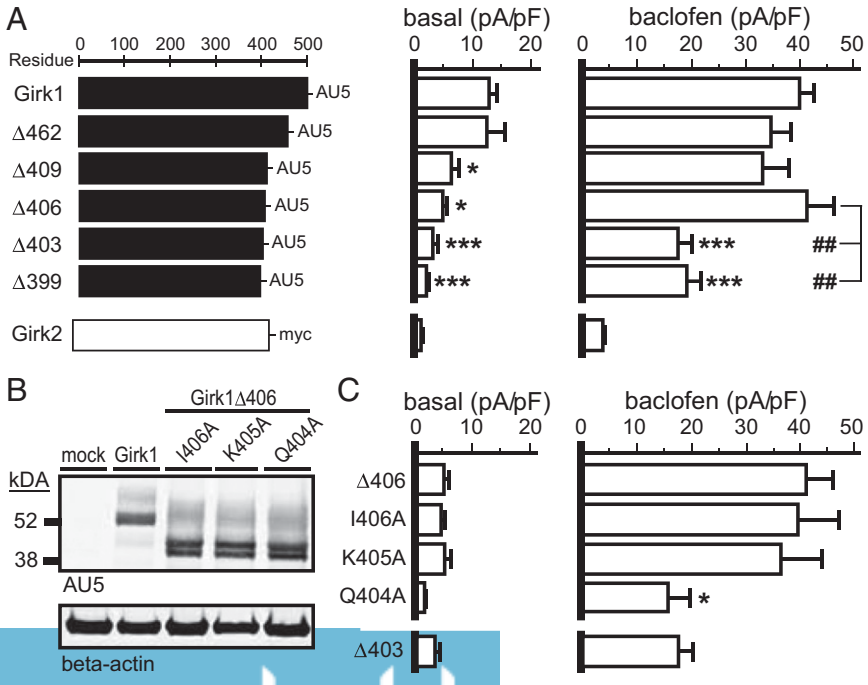

Fig. 2. Impact of the Girk1 distal C terminus. (*A*) Basal and baclofen-induced currents in cells expressing $GABA_BR$, Girk2, and the subunit depicted on the left (n = 12–61 per group). A significant impact of group was observed for basal ($F_{5,137}$ = 8.4; P < 0.001) and baclofen-induced ($F_{5,141}$ = 6.7; P < 0.001) currents. *P < 0.05 and ***P < 0.001 vs. Girk1/Girk2; ##P < 0.01 vs. Girk1Δ406/Girk2. Girk2 homomeric basal and baclofen-induced currents are shown for comparison but were not included in the analysis. (*B*) Immunoblot of I406A, K405A, and Q404A point mutants, generated on the Girk1Δ406 backbone. (*C*) Basal and baclofen-induced currents in cells expressing $GABA_BR$, Girk2, and the construct depicted on the left (n = 8–18 per group). A significant impact of group was observed for baclofen-induced ($F_{3,42}$ = 3.0; P < 0.05) but not basal ($F_{3,41}$ = 2.6; P = 0.06) current. *P < 0.05 vs. Girk1Δ406/Girk2.

Downloaded at Palestinian Territory, occupied on December 18, 2021
www.manaraa.com

induced currents were ~30% lower in cells expressing Girk1 (Q404A) (Fig. 3*A*). This difference was not related to reduced expression of Girk1(Q404A) (Fig. S3 *A* and *B*) or to a negative influence of Girk1(Q404A) on the protein level or surface trafficking of Girk2 (Fig. S3 *C* and *D*). The EC_{50} for baclofen activation of Girk1(Q404A)/Girk2 heteromers [0.76 μM; 95% confidence interval (CI): 0.52–1.11 μM], measured by sequential application of increasing baclofen concentrations (0.01–300 μM), was slightly but significantly greater ($F_{1,42} = 4.3$; $P < 0.05$) than that measured for Girk1/Girk2 (0.47 μM; 95% CI: 0.36–0.61). When coexpressed with Girk2 and Gβγ (Gβ$_1$ and Gγ$_2$), Girk1 and Girk1(Q404A) supported robust and indistinguishable Ba^{2+}-sensitive currents (Fig. 3 *B* and *C*). Collectively, these data are consistent with a role for Q404 in enhancing the channel–Gβγ interaction.

Impact of the Girk1 Core. Baclofen-induced currents observed for Girk1Δ399/Girk2 were significantly larger than those carried by Girk2 homomers ($t_{34} = 5.6$; $P < 0.001$), arguing that structures between residues 1 and 399 also contribute to the Girk1-dependent potentiation of Girk channel activity. To identify key structural elements within this larger region of Girk1, which contains domains critical for Girk channel function, we next generated three chimeras incorporating N-terminal (Girk1 residues 1–85), core (Girk1 residues 86–180), or C-terminal (Girk1 residues 181–501) domains from Girk1 within a Girk2 backbone and expressed them with Girk2 and $GABA_BR$ (Fig. 4). All three chimeras (NT, TM, CT) were expressed at higher levels than Girk1 (Fig. S4*A*), but none significantly altered the surface trafficking of Girk2 (Fig. S4*B*). Only the Girk1 core domain (TM) conferred a partial but significant potentiation of basal and baclofen-induced currents (Fig. 4*A*).

Single-channel conductance and mean open-time values are larger for Girk1-containing channels than Girk1-lacking counterparts (8, 14). Enhancement of these unitary properties should increase basal and receptor-induced whole-cell Girk currents. Thus, we next measured single-channel conductance and mean open times of baclofen-activated Girk channels in cells expressing Girk1/Girk2, Girk2 alone, or TM/Girk2. In cells expressing Girk1 and Girk2, most channel openings were reasonably well resolved (Fig. 4*B*), exhibiting a prominent single-channel conductance of 35 pS (Table 1 and Fig. S4*C*). The open-state dwell-time data for Girk1/Girk2 heteromers was modeled best with two terms (0.4 and 2.2 ms; Table 1 and Fig. S4*D*). In cells expressing Girk2 homomers, events were less well resolved; analysis revealed a single-channel conductance of 11 pS and a mean open time of 0.3 ms. Channels observed in cells expressing TM and Girk2 exhibited an intermediate

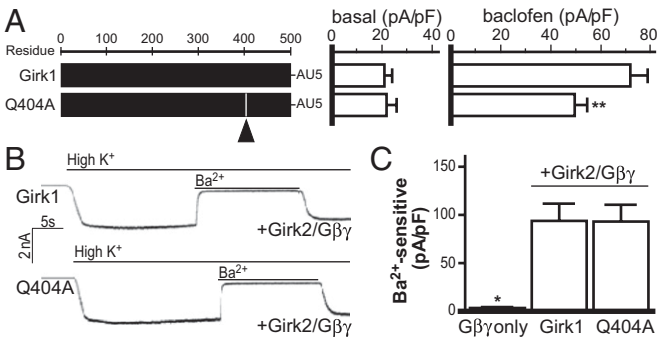

Fig. 3. Impact of Q404. (*A*) Basal and baclofen-induced currents in cells expressing $GABA_BR$, Girk2, and the depicted construct (n = 19–20 per group). A significant difference between groups was observed for baclofen-induced ($t_{37} = 2.8$; $P < 0.01$) but not basal ($t_{35} = 0.2$; $P = 0.9$) current. $^{**}P < 0.01$ vs. Girk1. (*B*) Ba^{2+}-sensitive currents measured in high-K^+ bath solution in cells expressing Gβ1γ2 and either Girk1/Girk2 or Girk1(Q404A)/Girk2 ($V_{hold} = -70$ mV). Bars denote the duration of Ba^{2+} (0.3 mM) application. (*C*) Summary of Ba^{2+}-sensitive currents in cells transfected with Gβ1γ2 and empty vector (Gβγ only), Girk1/Girk2, or Girk1(Q404A)/Girk2. A significant impact of group was observed ($F_{2,29} = 4.6$; $P < 0.05$). $^{*}P < 0.05$ vs. Girk1.

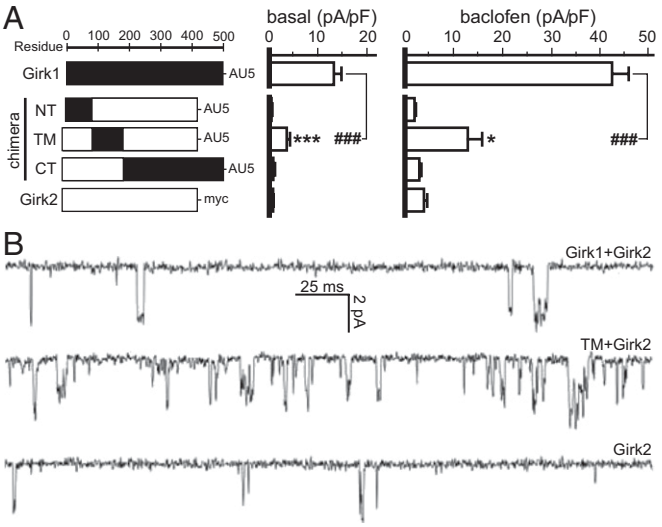

Fig. 4. Impact of the Girk1 core. (*A*) Basal and baclofen-induced currents in cells expressing $GABA_BR$, Girk2, and the depicted construct (n = 10–34 per group). A significant impact of group was observed for basal ($F_{5,105} = 10.3$; $P < 0.001$) and baclofen-induced ($F_{5,110} = 10.9$; $P < 0.001$) currents. $^{*}P < 0.05$ and $^{***}P < 0.001$ vs. Girk2 homomer; $^{\#\#\#}P < 0.001$ vs. Girk1/Girk2. (*B*) Representative segments (300 ms) of cell-attached recordings ($V_{hold} = -75$ mV), measured with 100 μM baclofen in the high-K^+ (150 mM) pipette solution, from cells expressing $GABA_BR$, Girk2, and either Girk1 (*Top*), TM chimera (*Middle*), or Girk2 (*Bottom*). A patch with higher activity (and at least 2 channels) is shown for TM to emphasize the profile overlap with Girk1/Girk2 heteromers and Girk2 homomers.

conductance (21 pS) and mean open times (0.4 and 1.7 ms), values significantly different from those of both Girk1/Girk2 heteromers and Girk2 homomers (Table 1). These data suggest that larger whole-cell currents seen in cells expressing TM/Girk2 compared with Girk2 homomers can be attributed, at least in part, to an enhancement of single-channel conductance and mean open time.

A second set of chimeras with overlapping Girk1 content was generated to better resolve potentiating elements within the 95-residue domain (Fig. 5). The three chimeras (M1-P, P, P-M2) were expressed at levels comparable to the TM chimera (Fig. S5 *A* and *B*). Single-channel conductance and open times were significantly lower for all three chimeras relative to TM but significantly greater than those for Girk2 homomers (Table 1). All three chimeras supported basal currents comparable to those measured for the TM chimera (Fig. 5*B*), implicating the Girk1 P-loop as a key potentiating influence on basal channel activity. Interestingly, baclofen-induced currents supported by the M1-P and P (but not P-M2) chimeras were significantly larger than those measured for the TM chimera, indicating that the Girk1 P-loop also enhances $GABA_BR$-Girk current and that this influence is tempered by structural content between Girk1 residues 150 and 180.

Six residues differ between Girk1 and Girk2 within this region, and all are found within the M2 domain (Fig. 5*A*). To identify the structural basis for the inhibitory influence of the M2 domain, we introduced Girk1-specific residues into the M2 domain of the P chimera, focusing on three substitutions predicted to exert the most significant structural impact (L173F, I175F, N184D). Whereas cells expressing $GABA_BR$, Girk2, and either P(I175F) or P(N184D) exhibited basal and baclofen-induced currents comparable to or greater than cells expressing the TM chimera, currents supported by the P(L173F) mutant were indistinguishable from those seen in cells expressing TM. Moreover, baclofen-induced currents in cells expressing P(L173F) were significantly lower than currents measured in cells expressing the P chimera (Fig. 5*C*). The single-channel conductance (but not mean open time) measured in cells coexpressing Girk2 and P(L173F) was also significantly lower than that measured for the P chimera (Table 1). Collectively, these data

Downloaded at Palestinian Territory, occupied on December 18, 2021
www.manaraa.com

Table 1. Summary of single-channel data

Subunit	Conductance, pS	Open time, ms
Girk1	35 ± 1	0.4 ± 0.5 (54%)
	22 ± 2	2.2 ± 0.4 (46%)
TM	21 ± 1*,†	0.4 ± 0.5 (49%)*,†
		1.7 ± 0.3 (51%)
M1-P	18 ± 1*,†,‡	0.2 ± 0.5 (56%)*,†,‡
		1.2 ± 0.3 (44%)
P	17 ± 1*,†,‡	0.5 ± 0.3 (64%)*,†,‡
		2.4 ± 0.5 (36%)
P-M2	17 ± 1*,†,‡	1.1 ± 0.1*,†,‡,§
P(L173F)	13 ± 1*,‡,§	0.9 ± 0.1*,†,‡
FAY	16 ± 1*,†,‡	0.2 ± 0.4 (60%)*,†,‡
		1.5 ± 0.3 (40%)
FA	13 ± 1*,‡,§	0.7 ± 0.2*,†,‡,§
S148F	14 ± 1*,‡,§	0.8 ± 0.1*,†,‡,§
T153A	14 ± 1*,‡,§	0.8 ± 0.2*,†,‡,§
V161Y	18 ± 1*,†	0.6 ± 0.1*,†,‡,§
Girk2	11 ± 1*	0.3 ± 0.2*,‡

Single-channel conductance and open times derived from channel events (n = 250–892) measured in three to five cells expressing Girk2 and the subunit listed on the left. Amplitude data were binned in a conventional histogram (0.2-pA bin width; 0.4- to 4.4-pA constraints), normalized, and fit using a Gaussian function. Models with different term number were compared automatically, and results from the optimal fit are listed here. Open-state dwell-time data were binned in a logarithmic histogram (15 bins per decade; 0.3- to 10-ms constraints). Square roots of bin counts were determined, and resultant histograms were fit using an exponential (log-probability) function. Optimal fits were determined for each channel. For two-term fits, the influence of each term is listed as a percentage. The Girk2(V142P) mutant was not evaluated because of low-level whole-cell activity. *P < 0.001 vs. Girk1/Girk2; †P < 0.05 vs. Girk2; ‡P < 0.05 vs. TM; §P < 0.05 vs. P.

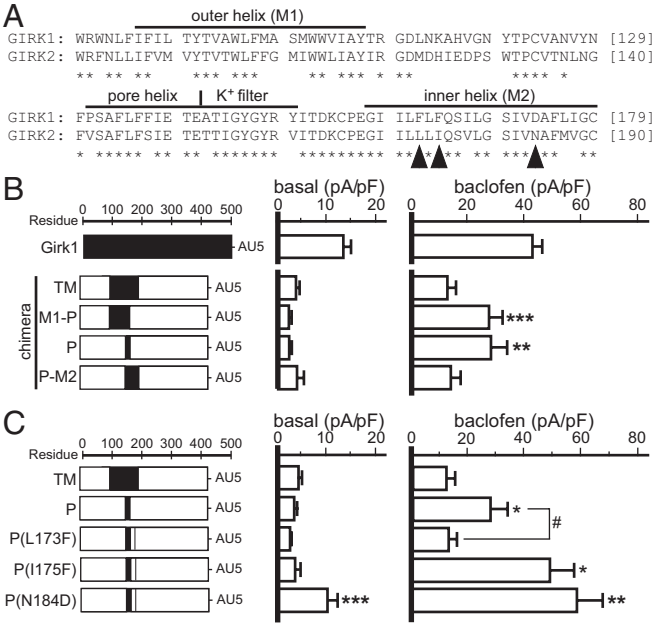

Fig. 5. Impact of the Girk1 P-loop and M2 domain. (*A*) Sequence alignment of Girk1 and Girk2 core domains, with key structural elements highlighted. The arrowheads denote three residues tested for their influence on the M2-dependent inhibition of baclofen-induced currents. (*B*) Basal and baclofen-induced currents in cells expressing $GABA_BR$, Girk2, and the depicted chimera (n = 12–22 per group). A significant impact of group was observed for baclofen-induced ($F_{3,54}$ = 7.6; P < 0.001) but not basal ($F_{3,55}$ = 1.0; P = 0.4) current. **P < 0.01 and ***P < 0.001 vs. TM. Basal and baclofen-induced currents for Girk1/Girk2 are presented for comparison but were not included in the statistical analysis. (*C*) Basal and baclofen-induced currents in cells expressing $GABA_BR$, Girk2, and the depicted construct (n = 7–22 per group). A significant impact of group was observed for baclofen-induced ($F_{4,55}$ = 15.6; P < 0.001) and basal ($F_{4,54}$ = 9.8; P < 0.001) currents. *P < 0.05 and **P < 0.01 vs. TM; #P < 0.05 vs. P.

suggest that residue F162 in the Girk1 M2 domain is a selective inhibitory influence on the receptor-dependent gating of heteromeric Girk channels.

Only four residues differ between Girk1 and Girk2 within the P-loop (Fig. 6*A*). To determine which residue(s) confers potentiation of basal and baclofen-induced currents, we generated Girk2 point mutants containing one or more Girk1 residues at the analogous positions. No enhancement of basal activity was observed when the single mutants were coexpressed with Girk2 (Fig. 6*C*). Girk2(S148F) did tend to support larger baclofen-induced currents, despite the fact that total protein levels for this mutant were significantly lower than Girk2 (Fig. S6). Mean open time for channels in cells expressing Girk2(S148F) and Girk2, however, was significantly longer than that of a Girk2 homomer, suggesting that the mutant was expressed and available to influence the unitary properties of the expressed channel.

We next evaluated the Girk2(S148F/T153A) double mutant, or FA mutant, reasoning that this dual substitution would promote a redistribution of intrasubunit interactions. T153 in Girk2 is located at the junction between the K^+-selectivity filter and pore helix (Fig. 6*B*), and it participates in an intrasubunit interaction with W106. Introduction of the Girk1-specific alanine at this position should preclude this interaction and foster an intrasubunit interaction between W106 and the Girk1-specific phenylalanine incorporated at position 148. Total expression levels of the FA mutant were, like Girk2(S148F), significantly lower than Girk2 (Fig. S6). Basal activity and unitary channel properties measured in cells expressing FA and Girk2 was comparable to those seen in cells expressing Girk2(S148F), and although baclofen-induced currents were larger than those measured in cells expressing Girk2 (S148F), the difference was not significant (Fig. 6*C*).

V142P and V161Y substitutions were next introduced independently to the FA mutant to generate PFA and FAY triple mutants. Introduction of the proline at position 142 should cause a premature termination of the pore helix, whereas the V161Y substitution should strengthen intersubunit interactions by promoting aromatic stacking with Y159 (conserved in all Girk subunits) in the adjacent Girk subunit (Fig. 6*B*). PFA protein levels were low in whole-cell extracts from transfected cells (Fig. S6), and PFA/Girk2 coexpression yielded basal and baclofen-induced responses comparable to those of Girk2 homomers. In contrast, total protein levels for FAY were notably higher than those of the PFA, FA, and S148F mutants (Fig. S6), and FAY/Girk2 coexpression recapitulated the enhanced basal and baclofen-induced currents seen with the P chimera (referred to as PFAY in Fig. 6*C*).

Importantly, reversal potentials for the baclofen-induced currents measured in the high-K^+ recording solution were similar ($F_{2,16}$ = 2.6; P = 0.1) for cells expressing Girk1/Girk2 (−42 ± 1 mV; n = 5), P/Girk2 (−33 ± 5 mV; n = 5), and FAY/Girk2 (−36 ± 1 mV; n = 7) and were close to the K^+ equilibrium potential (−43 mV). Thus, the potentiation of basal and baclofen-induced currents observed with P chimera and FAY mutant was not attributable to marked alterations in channel selectivity. Moreover, channels measured in cells expressing Girk2 and FAY or P chimera exhibited significantly longer mean open times and slightly larger single-channel conductances than Girk2 homomers, arguing that the potentiating influence of these P-loop residues on basal and baclofen-induced currents is mediated, at least in part, by an enhancement of unitary channel properties.

Discussion

Previous chimeric studies explored the influence of intracellular and core domains of Girk1 on channel function (14, 15, 16, 17), leading to the identification of N- and multiple C-terminal domains critical for promoting direct interactions with Gβγ, including the

Downloaded at Palestinian Territory, occupied on December 18, 2021
www.manaraa.com

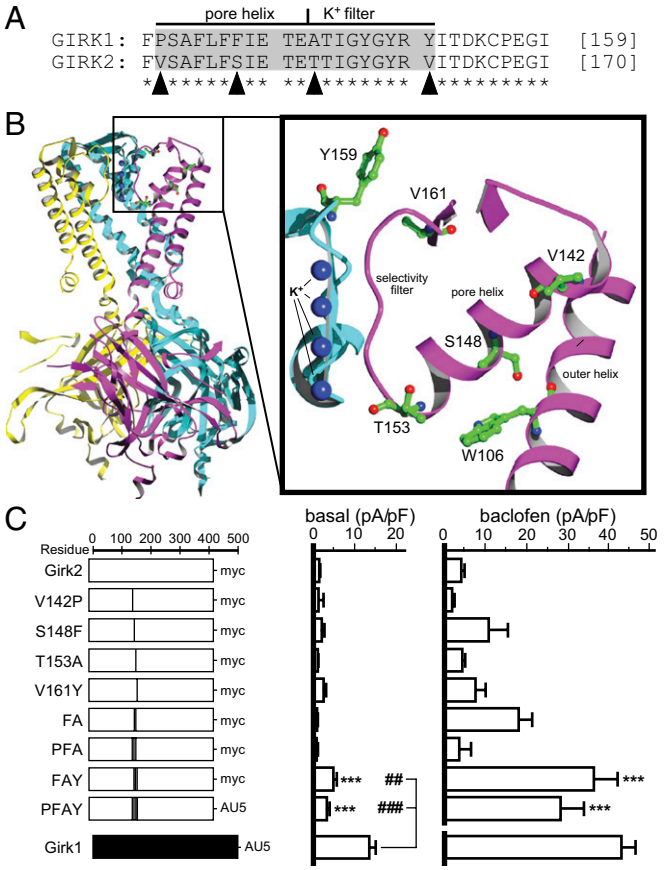

Fig. 6. Impact of Girk1 P-loop residues. (*A*) Alignment of Girk1 and Girk2 P-loop domains. The arrowheads denote the four amino acid differences between Girk1 and Girk2 in this domain. (*B*) Modeling of the Girk2 homomer [Protein Data Bank (PDB) ID code 3SYQ] in the open conformation, with one subunit (facing the viewer) removed for clarity. The three remaining subunits are displayed in different colors. (*Right*) Detailed structures within the pore, with the M2 domain (inner helix) of the fuchsia subunit removed for clarity. (*C*) Basal and baclofen-induced currents in cells expressing $GABA_BR$, Girk2, and the depicted construct ($n = 6$–17 per group). A significant impact of group was observed for basal ($F_{8,83} = 9.8$; $P < 0.001$) and baclofen-induced ($F_{8,81} = 14.1$; $P < 0.001$) currents. $^{***}P < 0.001$ vs. Girk2 homomer; $^{\#\#}P < 0.01$ and $^{\#\#\#}P < 0.001$ vs. Girk1/Girk2 heteromer (only select comparisons are shown).

"βL-βM sheet" (residues 331–340) and L333 (1). These structures form a binding pocket that maps onto the external face of an extended cytosolic ion permeation pathway (18). Given the conservation of these and other critical domains across Girk subunits, they cannot explain the potentiating influence of Girk1 on Girk currents. Moreover, whereas the distal C-terminal domain of Girk1 (residues 325–501) can confer enhanced Gβγ-dependent activation to a heteromeric channel consisting of Girk4 and an IRK1/Girk1 chimera, robust receptor-induced currents required the Girk1 core domain (15). Thus, structural features of Girk1 might enhance receptor-dependent Girk signaling via mechanisms that do not involve Gβγ binding.

Structural insights into the unique distal C-terminal domain of Girk1 are limited because published crystal structures were derived from recombinant proteins lacking the distal regions of the N- and C-terminal domains. Although this domain, alone, does not bind Gβγ, its presence significantly strengthened binding of Gβγ to the Girk1 C terminus (13). Thus, the potentiating effect of Girk1 on Girk-dependent signaling might reflect, in part, the presence of distal C-terminal domain that confers a stronger association between the channel and Gβγ. Here, we identified a single residue within this domain (Q404) that selectively influences receptor-induced Girk channel activity. Available evidence is consistent with the possibility that this residue strengthens the channel–Gβγ interaction. It is also possible, however, that Q404 strengthens the allosteric coupling that translates Gβγ binding to an increase in channel gating.

Three amino acids (F137, A142, Y150) in the P-loop were found to collaborate to enhance heteromeric channel activity, probably via the redistribution of intrasubunit interactions and strengthening of intersubunit interactions that leads to enhanced single-channel conductance and mean open time and, perhaps, enhanced gating. F137 was identified previously as an enhancer of basal and receptor-dependent currents carried by the Girk1/Girk4 heteromer (19). Although the precise structural impact of the phenylalanine substitution is unknown, manipulations at this site influence diverse channel properties. Indeed, an S148T substitution in Girk2 yields highly active homomeric channels (20). Perhaps more surprisingly, Girk1(F137S) homomers reach the cell surface and are functional, despite the lack of an endoplasmic reticulum export signal that precludes surface trafficking of Girk1 (21).

Our data show that the positive collective influence of F137, A142, Y150 on basal and receptor-induced Girk currents is tempered by F162 in the Girk1 M2 domain. Using the structure of the Girk2 homomer as a template, one would predict that replacing L173 (the analogous position in Girk2) with the relatively bulky phenylalanine would result in a Van der Waals interaction with I155 of the adjacent Girk subunit, pushing I155 toward the K^+-permeation pathway (Fig. S5*C*). In support of this contention, the unitary conductance of channels formed with P(L173F) was lower than that of the P chimera, and the longer mean open times (2.4 ms) observed with the P chimera were not seen for P(L173F). The relatively selective influence of this residue on receptor-dependent current argues that it is involved in conformational changes in the channel triggered by Gβγ binding.

Although pore-related structures that enhance unitary properties should increase basal (and receptor-dependent) whole-cell current, we found that the domain between 409 and 462 in the distal C terminus is a significant and selective determinant of receptor-independent channel activity. The impact of the distal C terminus of Girk1 on basal activity might relate to channel interactions with Gα subunits. $G\alpha_{i3}$ was found to interact with the distal Girk1 C terminus, leading to a reduction in basal activity and increased Gβγ-dependent activation of Girk1(F137S) homomers (22). In contrast, basal activity of Girk2 homomers was insensitive to $G\alpha_{i3}$-dependent modulation. In light of the substantial basal activity of Girk channels seen in neurons (e.g., ref. 23), refinement of the impact of the distal Girk1 C-terminal domain on basal activity is warranted.

The single-channel conductance and mean open time of Girk1-containing channels are both larger than those of Girk1-lacking channels. Our data reveal that Girk1 core domain accounts for much of the influence of Girk1 on mean open time and some of its influence on unitary conductance. Presumably, structures in the proximal N- and/or C-terminal domains of Girk1 that contribute to the cytoplasmic pore participate in modulating these unitary channel properties. Given the robust influence of Girk1 on Girk channel activity, it seems likely that Girk1 also enhances other aspects of channel function, including gating. In addition to an inner-helix gate formed by the second-transmembrane segments, Girk channels possess a G-loop gate found near the interface of the cytoplasmic domain and membrane (24). Binding of Gβγ to Girk2 homomers opens the G-loop gate in the absence of PIP_2 and both G-loop and inner-helix gates in the presence of PIP_2 (24). Although these gates are conserved across Girk subunits, Girk1 and Girk2 do differ with regard to PIP_2 affinity (25). Subunit-dependent differences in channel modulation by Na^+ also support the contention that subtle differences associated with Girk channel gates may translate into significant differences in channel activity (26).

The existence of four Girk subunit genes, and their overlapping but distinct expression patterns, suggests that subunit composition influences Girk channel function in tangible ways. Given the critical contributions made by Girk channels to complex behavior and

Downloaded at Palestinian Territory, occupied on December 18, 2021
www.manaraa.com

organ physiology (1), a detailed understanding of intrinsic and extrinsic factors that influence channel function is warranted. Here, we explored the structural underpinnings of the clearest Girk subunit-dependent functional difference described to date. These efforts have refined the map of features influencing receptor-dependent and independent activity of Girk1-containing channels, the dominant Girk channel type in the brain and heart.

Materials and Methods

Animals. Studies involving animals were approved by the University of Minnesota Institutional Animal Care and Use Committee. The generation of *Girk1*$^{-/-}$ mice was described previously (27).

Molecular Biology. pcDNA3-based expression constructs containing epitope-tagged rat Girk1 (Girk1-AU5) and mouse Girk2a (Girk2-myc) coding sequences served as parent constructs. Girk1 C-terminal deletion constructs were generated by PCR. Girk1/Girk2 chimeras were generated by overlap-extension PCR. Point mutations were introduced using the Quickchange II XL kit (Agilent Technologies). All constructs were validated by DNA sequencing. Expression constructs for human Gβ1 (FLAG-Gβ1) and Gγ2 (HA-Gγ2) were purchased from the Missouri S&T cDNA Resource Center.

Cell Culture and Biochemistry. For biochemical assays, HEK293FT cells (Invitrogen/Life Technologies) were transfected using the calcium phosphate technique and collected for analysis 36–54 h later. For electrophysiological studies, HEK293 cells (ATCC) were transfected with Lipofectamine LTX reagent (Invitrogen/Life Technologies); experiments were conducted 18–36 h later. Some cells were treated with pertussis toxin (Tocris Bioscience) for 12–18 h before electrophysiological characterization. Primary cultures of hippocampal neurons were prepared as described (28). For quantitative (q)RT-PCR and biotinylation studies, neurons were plated onto 3-cm Petri dishes and kept in culture for 10–12 d before experimentation. qRT-PCR conditions for *GABA$_B$R1* and *Girk2* were described previously (29).

Immunoblotting and HEK cell biotinylation experiments were performed as described (30). Blots were probed with primary antibodies targeting c-myc (11667149001; 1:500; Hoffmann-La Roche), β-actin (ab6276; 1:10,000; Abcam), AU5 (A190-227A; 1:1,000; Bethyl Laboratories), or Girk2 (APC-006; 1:200; Alomone Labs) and either donkey anti-mouse (926-32212; 1:7,000; LI-COR Biosciences) or anti-rabbit (926-68072; 1:7,000; LI-COR) secondary antibodies. Blots were developed and band intensities were quantified using the Odyssey Infrared imaging system (LI-COR).

Electrophysiology. Conditions for measuring baclofen-induced whole-cell Girk currents were described previously (28). Receptor-independent (basal) Girk current was determined by measuring the decrease in holding current in the high-K^+ bath solution evoked by 0.3 mM Ba^{2+}. Measured and command potentials were not corrected for liquid-junction potential. An Axopatch 200B patch-clamp amplifier (Molecular Devices) was used for measurement of cell-attached, single-channel activity. Borosilicate patch pipettes (4–6 MΩ) were filled with (in mM): 150 KCl, 1 $MgCl_2$, 5 EGTA/KOH, 5 Hepes/KOH, and 0.1 baclofen (pH 7.4). To zero the cell membrane potential, baclofen-induced single-channel activity was measured in a high-K^+ (150 mM) bath solution (in mM): 150 KCl, 1.8 $CaCl_2$, 0.5 $MgCl_2$, 5.5 D-glucose, 5 Hepes/KOH (pH 7.4). Effective zeroing of the membrane potential using this approach was validated by measuring the reversal potential of the high-conductance, weakly rectifying Trek1 (TWIK-related K^+ channel 1) K^+ channel. Immediately after gigaseal formation, membrane potential was clamped at −75 mV, recordings were low-pass–filtered at 2 kHz, sampled at 10 kHz, and stored on hard disk for analysis using pCLAMP Version 9.0 software. Analysis of single-channel conductance and mean open time was performed on 5- to 15-s recordings taken within the 30-s timeframe immediately following seal formation.

Data Analysis. Data are presented throughout as the means ± SEM. Statistical analyses were performed with Prism 5 (GraphPad Software). Group comparisons were typically made using Student's *t* test or one-way ANOVA followed by Tukey's honestly significant difference (HSD) post hoc test when appropriate. Open-state dwell-time data were analyzed using the Kolmogorov-Smirnoff test, while single-channel amplitude data were analyzed with the Kruskal Wallis test, with pairwise comparisons made using Dunn's multiple comparison test. In all analyses, the level of significance was set at $P < 0.05$.

ACKNOWLEDGMENTS. We thank Dr. Fang Li for help with structural interpretation and Dr. Jose Colón-Sáez and Joseph Patton for technical assistance. The work was supported by National Institutes of Health Grants MH061933, HL105550, and DA011806 (to K.W.) and T32 DA07234 (to K.M.).

1. Lüscher C, Slesinger PA (2010) Emerging roles for G protein-gated inwardly rectifying potassium (GIRK) channels in health and disease. *Nat Rev Neurosci* 11(5):301–315.
2. Lüscher C, Jan LY, Stoffel M, Malenka RC, Nicoll RA (1997) G protein-coupled inwardly rectifying K^+ channels (GIRKs) mediate postsynaptic but not presynaptic transmitter actions in hippocampal neurons. *Neuron* 19(3):687–695.
3. Karschin C, Dissmann E, Stühmer W, Karschin A (1996) IRK(1-3) and GIRK(1-4) inwardly rectifying K^+ channel mRNAs are differentially expressed in the adult rat brain. *J Neurosci* 16(11):3559–3570.
4. Signorini S, Liao YJ, Duncan SA, Jan LY, Stoffel M (1997) Normal cerebellar development but susceptibility to seizures in mice lacking G protein-coupled, inwardly rectifying K^+ channel GIRK2. *Proc Natl Acad Sci USA* 94(3):923–927.
5. Koyrakh L, et al. (2005) Molecular and cellular diversity of neuronal G-protein-gated potassium channels. *J Neurosci* 25(49):11468–11478.
6. Lesage F, et al. (1995) Molecular properties of neuronal G-protein-activated inwardly rectifying K^+ channels. *J Biol Chem* 270(48):28660–28667.
7. Inanobe A, et al. (1999) Molecular cloning and characterization of a novel splicing variant of the Kir3.2 subunit predominantly expressed in mouse testis. *J Physiol* 521(Pt 1):19–30.
8. Krapivinsky G, et al. (1995) The G-protein-gated atrial K^+ channel I_{KACh} is a heteromultimer of two inwardly rectifying K(+)-channel proteins. *Nature* 374(6518):135–141.
9. Kofuji P, Davidson N, Lester HA (1995) Evidence that neuronal G-protein-gated inwardly rectifying K^+ channels are activated by G beta gamma subunits and function as heteromultimers. *Proc Natl Acad Sci USA* 92(14):6542–6546.
10. Duprat F, et al. (1995) Heterologous multimeric assembly is essential for K^+ channel activity of neuronal and cardiac G-protein-activated inward rectifiers. *Biochem Biophys Res Commun* 212(2):657–663.
11. Fowler CE, Aryal P, Suen KF, Slesinger PA (2007) Evidence for association of GABA(B) receptors with Kir3 channels and regulators of G protein signalling (RGS4) proteins. *J Physiol* 580(Pt 1):51–65.
12. Wiser O, et al. (2006) Modulation of basal and receptor-induced GIRK potassium channel activity and neuronal excitability by the mammalian PINS homolog LGN. *Neuron* 50(4):561–573.
13. Huang CL, Jan YN, Jan LY (1997) Binding of the G protein betagamma subunit to multiple regions of G protein-gated inward-rectifying K^+ channels. *FEBS Lett* 405(3):291–298.
14. Stevens EB, Woodward R, Ho IH, Murrell-Lagnado R (1997) Identification of regions that regulate the expression and activity of G protein-gated inward rectifier K^+ channels in Xenopus oocytes. *J Physiol* 503(Pt 3):547–562.
15. Slesinger PA, Reuveny E, Jan YN, Jan LY (1995) Identification of structural elements involved in G protein gating of the GIRK1 potassium channel. *Neuron* 15(5):1145–1156.
16. Chan KW, Sui JL, Vivaudou M, Logothetis DE (1997) Specific regions of heteromeric subunits involved in enhancement of G protein-gated K^+ channel activity. *J Biol Chem* 272(10):6548–6555.
17. Kunkel MT, Peralta EG (1995) Identification of domains conferring G protein regulation on inward rectifier potassium channels. *Cell* 83(3):443–449.
18. Nishida M, MacKinnon R (2002) Structural basis of inward rectification: Cytoplasmic pore of the G protein-gated inward rectifier GIRK1 at 1.8 A resolution. *Cell* 111(7):957–965.
19. Chan KW, Sui JL, Vivaudou M, Logothetis DE (1996) Control of channel activity through a unique amino acid residue of a G protein-gated inwardly rectifying K^+ channel subunit. *Proc Natl Acad Sci USA* 93(24):14193–14198.
20. Rogalski SL, Appleyard SM, Pattillo A, Terman GW, Chavkin C (2000) TrkB activation by brain-derived neurotrophic factor inhibits the G protein-gated inward rectifier Kir3 by tyrosine phosphorylation of the channel. *J Biol Chem* 275(33):25082–25088.
21. Ma D, et al. (2002) Diverse trafficking patterns due to multiple traffic motifs in G protein-activated inwardly rectifying potassium channels from brain and heart. *Neuron* 33(5):715–729.
22. Rubinstein M, Peleg S, Berlin S, Brass D, Dascal N (2007) Galphai3 primes the G protein-activated K^+ channels for activation by coexpressed Gbetagamma in intact Xenopus oocytes. *J Physiol* 581(Pt 1):17–32.
23. Chen X, Johnston D (2005) Constitutively active G-protein-gated inwardly rectifying K^+ channels in dendrites of hippocampal CA1 pyramidal neurons. *J Neurosci* 25(15):3787–3792.
24. Whorton MR, MacKinnon R (2011) Crystal structure of the mammalian GIRK2 K^+ channel and gating regulation by G proteins, PIP_2, and sodium. *Cell* 147(1):199–208.
25. Thomas AM, Brown SG, Leaney JL, Tinker A (2006) Differential phosphoinositide binding to components of the G protein-gated K^+ channel. *J Membr Biol* 211(1):43–53.
26. Ho IH, Murrell-Lagnado RD (1999) Molecular determinants for sodium-dependent activation of G protein-gated K^+ channels. *J Biol Chem* 274(13):8639–8648.
27. Bettahi I, Marker CL, Roman MI, Wickman K (2002) Contribution of the Kir3.1 subunit to the muscarinic-gated atrial potassium channel I_{KACh}. *J Biol Chem* 277(50):48282–48288.
28. Xie K, et al. (2010) Gbeta5 recruits R7 RGS proteins to GIRK channels to regulate the timing of neuronal inhibitory signaling. *Nat Neurosci* 13(6):661–663.
29. Arora D, et al. (2011) Acute cocaine exposure weakens GABA(B) receptor-dependent G-protein-gated inwardly rectifying K^+ signaling in dopamine neurons of the ventral tegmental area. *J Neurosci* 31(34):12251–12257.
30. Mirkovic K, Wickman K (2011) Identification and characterization of alternative splice variants of the mouse *Trek2/Kcnk10* gene. *Neuroscience* 194:11–18.

Downloaded at Palestinian Territory, occupied on December 18, 2021
www.manaraa.com